The role of packing effects at the liquid-solid interface: a model for a surface phase transition

1990 J. Phys.: Condens. Matter 2 3081

(http://iopscience.iop.org/0953-8984/2/13/018)

J. Phys.: Condens. Matter 2 (1990) 3081–3092. Printed in the UK

The role of packing effects at the liquid–solid interface: a model for a surface phase transition

E Kierlik and M L Rosinberg
Laboratoire de Structure et Reactivité aux Interfaces, Université Pierre et Marie Curie, Bâtiment F, 4 place Jussieu 75230, Paris Cédex 05, France

Received 6 July 1989, in final form 27 October 1989

Abstract. We present theoretical and computer simulation results for the structure of a hard-sphere fluid adsorbed onto a lattice of attractive sites placed on a planar hard wall. It is shown that packing effects in the dense fluid may induce a structural phase transition in the adsorbed layer. This transition is predicted by a theory which relates the properties of the interface to those of a 2D lattice gas with an effective interaction potential.

1. Introduction

In recent work [1], it has been predicted that packing effects may induce a structural phase transition in the first layer of a liquid adsorbed onto a solid substrate with a periodic structure. The prediction was made for a simple model of localised adsorption in which the liquid was represented by a hard-sphere fluid and the solid by a flat surface with sticky (i.e. adhesive) adsorption sites placed on a periodic lattice. The theory was based on an exact isomorphism between the original three-dimensional (3D) adsorption model and a fictitious two-dimensional (2D) lattice gas, and it elucidated how the presence of a dense liquid with a hard-core exclusion between the particles originated an effective attractive potential in the 2D lattice gas. Because of this attractive potential, gas–liquid condensation, corresponding to a mobile–localised phase transition in the first layer of the liquid, could occur for some value of the stickiness of the sites. However, in a subsequent Monte Carlo (MC) simulation [2], such a discontinuous behaviour of the coverage was not observed. In this simulation, the sticky potential was replaced for technical reasons by a constant and negative potential inside a small cylindrical volume centred around each site. The correspondence between these two potentials was obtained by equating their second virial coefficients. While this new potential retained two important characteristics of the sticky potential—attraction of a site was limited to the spheres very close to the wall and only one sphere could be adsorbed—the choice of the parameters for the lattice and the adsorption potential made in [2] introduced an undesirable steric effect: a particle adsorbed on a site could prevent another particle from moving onto an adjacent site. Is this effect sufficient to hinder the transition or is the theoretical prediction incorrect? We note that in [1] the statistical treatment of the lattice gas was only approximate (limitation to pair interactions between nearest neighbours (NNs) and mean-field approximation). On the other hand, in the case of adsorption onto a structureless solid (mobile adsorption), we have shown recently

0953-8984/90/133081 + 12 $03.50

[3] that such an 'effective 2D' theory yields results in reasonable agreement with MC simulation and better than those provided by other theoretical approaches (Percus–Yevick theory or density functional).

The aim of the present paper is thus to revisit the problem both theoretically and numerically and to find under which circumstances the transition can occur. The paper is arranged as follows. In section 2, we extend the theory of [1] to include the more realistic potential used in the simulation and we discuss the conditions needed to observe the transition. We then verify that these were not realised in the simulation performed in [2]. In section 3, we report our own MC simulation results, now performed with theoretically favourable conditions. The main result of our computation is the discontinuous variation in the fraction of sites occupied and the total adsorption as a function of the strength of the site–particle potential. We conclude with a brief discussion of the influence of n-body effects in the interface.

2. Adsorption model and effective 2D theory

We consider a fluid of hard spheres with hard-core diameter σ, in contact with a reservoir at fixed μ, T, near a hard wall placed at $z = -\sigma/2$ (i.e. the centres of the particles are limited to the region $z > 0$). The adsorbing potential is defined by

$$-\beta v(\boldsymbol{r}) = \begin{cases} \beta\varepsilon & 0 < z < \delta \qquad |\boldsymbol{R} - \boldsymbol{R}_\alpha| < a \\ 0 & \text{elsewhere} \end{cases} \tag{1}$$

where $\beta = (kT)^{-1}$, $\boldsymbol{r} = (\boldsymbol{R}, z)$ denotes the position of a fluid particle and $\boldsymbol{R}_\alpha = (x_\alpha, y_\alpha)$ the position of a site on the wall (all sites are equivalent). The sites are placed on a 2D lattice, with NN distance d. We assume that $\delta \ll \sigma$, $a \ll \sigma$ and $d \geqslant \sigma$. With these conditions, the characteristic function of a site $\chi_\alpha(\boldsymbol{r}) = \Theta(\delta - z)\Theta(a - |\boldsymbol{R} - \boldsymbol{R}_\alpha|)$, where Θ is the Heaviside step function, verifies that

$$\chi_\alpha(\boldsymbol{r})\chi_\beta(\boldsymbol{r}) = 0 \qquad \text{if } \alpha \neq \beta. \tag{2}$$

We then define the adsorbed layer as the set of molecules having their centres inside the potential wells. Quantities of interest to our study are the fraction θ of sites occupied, the total adsorption Γ with respect to the wall boundary and the surface excess grand potential ω^s per unit wall area: $\omega^s = \Omega^s/A$. From thermodynamics we have

$$\Gamma = \frac{1}{A}\int_{z>0} [\rho(\boldsymbol{r}) - \rho_b]\,\mathrm{d}\boldsymbol{r} = -\frac{\partial \omega^s}{\partial \mu} \tag{3a}$$

$$\theta = -(1/\tau)(\partial \omega^s/\partial \varepsilon) \tag{3b}$$

where ρ_b is the bulk density and τ the density of sites on the surface.

We now develop the same procedure used in [1, 3]. We start from the grand partition function of the system given by

$$\Xi = \sum_n \frac{z^n}{n!}\int \exp(-\beta H_0)\prod_i \exp\left[\beta\varepsilon\left(\sum_\alpha \chi_\alpha(\boldsymbol{r}_i)\right)\right]\mathrm{d}\boldsymbol{r}^n \tag{4}$$

where H_0 is the Hamiltonian for $\varepsilon = 0$, i.e. the hard-sphere–hard-wall (HS-HW) interface, and z the activity of the fluid. Introducing the Mayer function

$$f_i = \exp\left[\beta\varepsilon\left(\sum_\alpha \chi_\alpha(\boldsymbol{r}_i)\right)\right] - 1 = [\exp(\beta\varepsilon) - 1]\left(\sum_\alpha \chi_\alpha(\boldsymbol{r}_i)\right) \tag{5}$$

where (2) has been used, and expanding (4) in powers of $\exp(\beta\varepsilon) - 1$, we find after some manipulations that

$$\frac{\Xi}{\Xi_0} = \sum_n \frac{1}{n!}[\exp(\beta\varepsilon) - 1]^n \int \rho_0^{(n)}(1, 2, \ldots, n) \prod_i^n \left(\sum_\alpha \chi_\alpha(r_i) \right) \mathrm{d}r^n \tag{6}$$

where Ξ_0 and $\rho_0^{(n)}(1, 2, \ldots, n)$ are respectively the grand partition function and the n-particle density in the HS–HW interface. So far, all equations are exact. As in [1, 3], we now introduce a first approximation; we assume that the n-particle distribution functions

$$g_0^{(n)}(\boldsymbol{r}^n) = \rho_0^{(n)}(\boldsymbol{r}^n) \Big/ \prod_i^n \rho_0(z_i)$$

are independent of z in the region $0 < z < \delta$:

$$g_0^{(n)}(\boldsymbol{r}_1, \boldsymbol{r}_2, \ldots, \boldsymbol{r}_n) = g_0^{(n)}(\boldsymbol{R}_1, 0; \boldsymbol{R}_2, 0; \ldots; \boldsymbol{R}_n, 0). \tag{7}$$

This seems reasonable since $\delta \ll \sigma$ (see, however, the remark after equation 5.11 in [3]).

Then we get

$$\frac{\Xi}{\Xi_0} = \sum_n \frac{1}{n!} \left(\frac{\lambda \rho_0^{\mathrm{av}}}{\pi a^2} \right)^n \int \exp[-\beta w_0^{(n)}(\boldsymbol{R}^n)] \prod_i^n \left(\sum_\alpha \Theta(a - |\boldsymbol{R}_i - \boldsymbol{R}_\alpha|) \right) \mathrm{d}\boldsymbol{R}^n \tag{8}$$

where $\lambda = \pi a^2 \delta[\exp(\beta\varepsilon) - 1]$, $\rho_0^{\mathrm{av}} = (1/\delta)\int_0^\delta \rho_0(z)\,\mathrm{d}z$, and $w_0^{(n)}(\boldsymbol{R}^n)$ is the n-body potential of mean force on the surface defined by $g_0^{(n)}(\boldsymbol{R}_1, 0; \boldsymbol{R}_2, 0; \ldots; \boldsymbol{R}_n, 0) = \exp[-\beta w_0^{(n)}(\boldsymbol{R}^n)]$. Therefore, as in [1, 3], Ξ/Ξ_0 identifies to the grand partition function of a 2D fluid characterised by the fugacity $z_{2\mathrm{D}} = \lambda \rho_0^{\mathrm{av}}/\pi a^2$ and by the many-body potentials $w_0^{(n)}(\boldsymbol{R}^n)$. The 2D density $\theta_{2\mathrm{D}} = (1/A\tau)\{\partial[\ln(\Xi/\Xi_0)]/\partial(\ln\lambda)\}$ is related to the 'real' fraction θ of sites occupied by the simple relation

$$\theta_{2\mathrm{D}} = [1 - \exp(-\beta\varepsilon)]\theta \tag{9}$$

where (3*b*) has been used.

However, at this point, a difficulty remains: Ξ/Ξ_0 cannot be identified with the grand partition function of a 2D lattice gas since particles may move in small disks around the sites. Therefore, without any additional assumptions, all the benefit of the sticky case [1, 4], where results from the 2D Ising model can be used, is lost. We then introduce a generalised Kirkwood superposition approximation for the n-particle distribution functions at the HS–HW interface

$$g_0^{(n)}(1, 2, \ldots, n) = \prod_{i<j}^n g_0^{(2)}(i, j) \tag{10}$$

so that we are left only with pairwise interactions in Ξ/Ξ_0:

$$\frac{\Xi}{\Xi_0} = \sum_n \frac{1}{n!} \left(\frac{\lambda \rho_0^{\mathrm{av}}}{\pi a^2} \right)^n \int \exp\left(-\beta \sum_{i<j} w_0^{(2)}(\boldsymbol{R}_i, \boldsymbol{R}_j) \right) \prod_i^n \left(\sum_\alpha \Theta(a - |\boldsymbol{R}_i - \boldsymbol{R}_\alpha|) \right) \mathrm{d}\boldsymbol{R}^n. \tag{11}$$

Then, as we have included in ρ_0^{av} the z-dependence due to the finite value of δ, we try to eliminate the R-dependence due to the finite extent of the sites on the surface by introducing an average pair distribution function

$$g_0^{\mathrm{av}}(\boldsymbol{R}_\alpha, \boldsymbol{R}_\beta) = \frac{1}{(\pi a^2)^2} \int g_0^{(2)}(\boldsymbol{R}, 0; \boldsymbol{R}', 0) \Theta(a - |\boldsymbol{R} - \boldsymbol{R}_\alpha|) \Theta(a - |\boldsymbol{R}' - \boldsymbol{R}_\beta|)\,\mathrm{d}\boldsymbol{R}\,\mathrm{d}\boldsymbol{R}'. \tag{12}$$

If we assume that

$$\left(\frac{1}{\pi a^2} \right)^n \int \mathrm{d}\boldsymbol{R}^n \prod_{i<j}^n g_0^{(2)}(\boldsymbol{R}_i, 0; \boldsymbol{R}_j, 0) \prod_i^n \Theta(a - |\boldsymbol{R}_i - \boldsymbol{R}_{\alpha_i}|) = \prod_{i<j}^n g_0^{\mathrm{av}}(\boldsymbol{R}_{\alpha_i}, \boldsymbol{R}_{\alpha_j}) \tag{13}$$

we finally obtain

$$\frac{\Xi}{\Xi_0} = \sum_n \frac{1}{n!}(\lambda\rho_0^{av})^n \Big[\sum_{\text{all sites}} \exp\Big(-\beta \sum_{i<j} w_0^{av}(\boldsymbol{R}_{\alpha_i}, \boldsymbol{R}_{\alpha_j})\Big)\Big] \tag{14}$$

where $w_0^{av}(\boldsymbol{R}_\alpha, \boldsymbol{R}_\beta) = -kT \ln[g_0^{av}(\boldsymbol{R}_\alpha, \boldsymbol{R}_\beta)]$. Ξ/Ξ_0 is now isomorphic to the grand partition function of a 2D lattice gas.

The approximation (13), which affects all terms in Ξ/Ξ_0 beyond the order 2 in λ, is quite unverifiable. However, from the mathematical point of view, it seems all the more justified as the spatial extent of the sites is small and the function $g_0^{(2)}$ varies smoothly outside the core. In particular, it becomes exact in the sticky limit [1] or in the 'Langmuirian' case when particles adsorbed on different sites do not interact, i.e. $g_0^{(2)}(\boldsymbol{R}_i, 0; \boldsymbol{R}_j, 0) = 0$ if $|\boldsymbol{R}_i - \boldsymbol{R}_j| < d - 2a$ and $g_0^{(2)}(\boldsymbol{R}_i, 0; \boldsymbol{R}_j, 0) = 1$ elsewhere. In this case one gets from (11) the simple 'isotherm' equation

$$\lambda\rho_0^{av} = \theta_{2D}(1 - \theta_{2D})^{-1}. \tag{15}$$

We may also remark that the average potential $w_0^{av}(\boldsymbol{R}_\alpha, \boldsymbol{R}_\beta)$ appears quite naturally in the first-order perturbation theory with respect to the Mayer function $f(\boldsymbol{R}, \boldsymbol{R}') = \exp[-\beta w_0^{(2)}(\boldsymbol{R}, \boldsymbol{R}')] - 1$. Indeed one then gets from (11) the isotherm

$$\lambda\rho_0^{av} = \theta_{2D}(1 - \theta_{2D})^{-1} \exp\Big(-\frac{\theta_{2D}}{(\pi a^2)^2} \sum_\beta \times \int f(\boldsymbol{R}, \boldsymbol{R}')\Theta(a - |\boldsymbol{R} - \boldsymbol{R}_\alpha|)\Theta(a - |\boldsymbol{R}' - \boldsymbol{R}_\beta|)\, d\boldsymbol{R}\, d\boldsymbol{R}'\Big) \tag{16}$$

which can be written as

$$\lambda\rho_0^{av} = \theta_{2D}(1 - \theta_{2D})^{-1} \exp\Big\{-\theta_{2D} \sum_\beta \Big[\exp\Big(\frac{-w_0^{av}(\boldsymbol{R}_\alpha, \boldsymbol{R}_\beta)}{kT}\Big) - 1\Big]\Big\} \tag{17}$$

and, expanding again the exponential to first order, one finds that

$$\lambda\rho_0^{av} = \theta_{2D}(1 - \theta_{2D})^{-1} \exp\Big(\beta\theta_{2D} \sum_\beta w_0^{av}(\boldsymbol{R}_\alpha, \boldsymbol{R}_\beta)\Big) \tag{18}$$

which can be also derived directly from (14) by using the classical mean field (Bragg–Williams) approximation.

On the other hand, if we only consider in (14) the contribution coming from NN sites (i.e. if $w_0^{av}(\boldsymbol{R}_\alpha, \boldsymbol{R}_\beta)$ becomes negligible for pair of particles which are not adsorbed on NN sites), we may use the exact results of the 2D Ising model for a qualitative discussion of the possibility of liquid–gas condensation in the lattice gas. The critical value of the NN interaction potential at fixed T will of course depend on the type of lattice: for instance one has $\exp[-\beta w_0^{av}(d)]|_{crit} = g_0^{av}(d)|_{crit} = 3 + 2\sqrt{2}$ for the square lattice and 3 for the triangular lattice [5]. Since $g_0^{(2)}(|\boldsymbol{R} - \boldsymbol{R}'|; 0; 0)$ can be obtained with a good accuracy using the Plischke–Henderson parametrisation [6] with $g_0^{(2)}$(bulk) given by Verlet–Weis [7], we now have a way to determine approximately the conditions on ρ_b and on the geometry of the adsorption lattice (d, a) for the existence of the transition. g_0^{av} defined by (12) can be easily calculated by a 2D integration

$$g_0^{av}(R_{\alpha\beta}) = \int_0^{\pi/2} dx \int_0^{2\pi} dy\, g_0^{(2)}[R_{\alpha\beta}^2 + a^2\cos^2(x) + 2aR_{\alpha\beta}\cos(x)\cos(y); 0; 0][x - 0.5\sin(2x)]\sin(2x). \tag{19}$$

We first find that in the square lattice no transition can occur at normal liquid density,

whatever the values of d and a, because there are too few NNs. In the triangular lattice, which is the one considered in [1] and [2], the largest value of $g_0^{av}(d)$ for ρ_b and a fixed, is obtained for $d = \sigma + 2a$ (in the sticky limit ($a = 0$) this is a sort of 'epitaxial' condition and one reaches the critical value $g_0^{av}(d) = 3$ for $\rho_b\sigma^3 = 0.672$). On the other hand, for ρ_b and d fixed, $g_0^{av}(d)$ is a decreasing function of the site radius a. These results are a clear consequence of the steric effects noted in the introduction and therefore they invalidate the conclusion of [2]: the spatial extent of the adsorption sites is unfavourable to the localisation of the particles. This is because the spatial average in (12) includes the hard-core region in which $g_0^{(2)}(R; 0; 0) = 0$. Of course, such an effect disappears if $d > \sigma + 2a$. Unfortunately, this condition was never realised in the simulations performed in [2] and we can verify that $g_0^{av}(d)$ never reached the critical value 3.

Incidentally, we remark that $g_0^{av}(d) = 1.05$ (i.e. $w_0^{av}(d) \simeq 0$) for the simulation performed with $\rho_b\sigma^3 = 0.78$, $d = 1.1\sigma$ and $a = 0.4\sigma$ so that we may expect that the Langmuir or the Bragg–Williams approximations (15) and (18) become valid. Indeed we see in figure 1 that the agreement of the MC result with the theoretical prediction is good in the full range of variation of $\beta\varepsilon$ (note from (9) that θ_{2D} identifies with θ only for large $\beta\varepsilon$ and that $\theta \neq 0$ for $\beta\varepsilon = 0$). For the other cases studied in [2], such an agreement is only obtained in the domain of low θ.

3. Monte Carlo simulations

3.1. Method

From the preceding discussion it is clear that, even at a large bulk density, a small size for the sites is a necessary condition for observing the transition. On the other hand, if the radius a is too small, particles will never be adsorbed after a reasonable number of MC steps. Thus we chose the following conditions for our simulation: $\eta_b = \pi/6\rho_b\sigma^3 = 0.46$, $\delta = 0.1\sigma$, $a = 0.025\sigma$ and $d = 1.05\sigma$. These parameters ensure the value $g_0^{av}(d) = 3.6$ for the triangular lattice.

The simulation cell was a parallelepipedic volume with lateral dimensions $L_x = 16d$, $L_y = 8d\sqrt{3}$ and standard boundary conditions imposed in the x and y directions. The two adsorbing walls were located at $z = \pm L_z/2$ and each contained 256 sites. The total number of particles was $N = 4155$ and L_z was guessed as in [3] in order to obtain the desired bulk density in the central region $(-L_z/8, L_z/8)$. After the usual initialisation procedure [2, 3], we started the simulation from two different initial equilibrium configurations S_1 ($L_z = 18.5\sigma$) and S_2 ($L_z = 18\sigma$), corresponding respectively to $\beta\varepsilon = 0$ and $\beta\varepsilon = \infty$. We then gradually decreased or increased $\exp(-\beta\varepsilon)$ to obtain two series of configurations from S_1 or S_2, respectively (in contrast with [3] we did not find it necessary to vary L_z with $\beta\varepsilon$, since Γ remained virtually constant in each thermodynamical branch, as we shall see below). No metastability was observed near $\varepsilon = \infty$ and we always obtained $\theta(\infty) = 1$, the expected thermodynamical value (this was not always the case in [2] because of the steric effects discussed above). Moreover, the localisation of the particles on well defined sites with $d = 1.05\sigma$ hindered the occurrence of the incommensurate intrinsic 2D ordering observed in the non-localised case [3]. For each value of ε and the two series of configurations, equilibrium was decided to be achieved when the values of θ were stable and equal on the two adsorbing planes in the limit of statistical fluctuations. A typical equilibration required 10^4 trial moves per particle. Averages were then calculated with 2×10^4 additional moves per particle. Since the adatoms (those particles which are on the sites) are not the only ones having their centres in the range $0 < z < \delta$, we evaluated two different pair distribution functions: the site–site distribution function

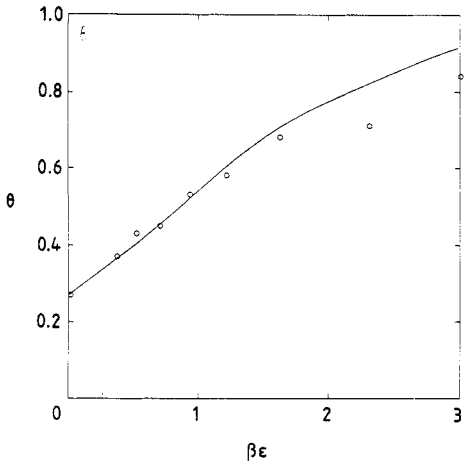

Figure 1. The fraction of sites occupied as a function of the site potential for $\rho_b\sigma^3 = 0.78$, $\delta = 0.2\sigma$, $d = 1.1\sigma$ and $a = 0.4\sigma$. Comparison between MC results [2] (○) and the Bragg–Williams approximation (18) (——).

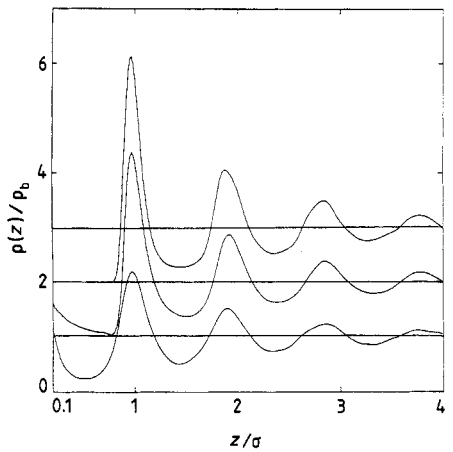

Figure 2. The normalised density profile $\rho(z)/\rho_b$ outside the adsorbed layer ($z > \delta$): MC results for different values of the site potential. From bottom to top, $\exp(-\beta\varepsilon) = 1, 0.05$ and 0 (the lowest curve remains almost unchanged up to $\exp(-\beta\varepsilon) = 0.06$).

$g_{ss}(\alpha, \beta)$, obtained by counting the pairs of adatoms, and the in-plane radial distribution function $g_r(R)$ defined as

$$\iint \rho^{(2)}(\boldsymbol{R}', \boldsymbol{R}'')\delta(|\boldsymbol{R}' - \boldsymbol{R}''| - R)\,\mathrm{d}\boldsymbol{R}'\,\mathrm{d}\boldsymbol{R}'' \left[\iint \rho(\boldsymbol{R}')\rho(\boldsymbol{R}'')\,\mathrm{d}\boldsymbol{R}'\,\mathrm{d}\boldsymbol{R}''\right]^{-1}$$

and obtained by counting all pairs of particles in the region $0 < z < \delta$. It can be shown easily from (8) that in the 2D picture $g_{ss}(\alpha, \beta)$ can be identified with the pair distribution function of the 2D fluid. Note also that none of these functions describes the structure of the whole first layer which is in general broader (see below). Also determined in the simulation are the density profile $\rho(z) = (1/L_xL_y)\int\rho(\boldsymbol{R}, z)\,\mathrm{d}\boldsymbol{R}$, and the probability $P_\varepsilon(l)$ for fixed ε of a configuration with l occupied sites [2].

3.2. Results and discussion

The MC normalised density profile $\rho(z)/\rho_b$ outside the adsorbed layer ($z > \delta$) is shown in figure 2 for several values of ε ($\rho(z)$ decreases steeply between $z = 0$ and $z = 0.1\sigma$ and the values inside this layer are too large to be represented on the same scale; one has respectively $\rho(0)/\rho_b = 10.3$, 14.9 and 17.1 at contact with the wall for $\exp(-\beta\varepsilon) = 1, 0.05$ and 0). Results for the thermodynamical quantities θ, Γ and for the mean square fluctuations of θ are summarised in table 1. Also given in this table are the average numbers of particles per unit area in the first and second layers, which we define respectively by $m_1 = \int_0^{z_0}\rho(z)\,\mathrm{d}z$ and $m_2 = \int_{z_0}^{z_1}\rho(z)\,\mathrm{d}z$, where $z_0(\varepsilon)$ and $z_1(\varepsilon)$ are the locations of the first and second minima in the density profile.

The main result of our simulation is the sharp variation in θ, Γ and m_1 observed near $\beta\varepsilon = 2.9 \pm 0.1$. This result may be considered as the signature of the first-order transition predicted in section 2. As usual, such a first-order transition also appears via the occurrence of hysteresis and metastability due to a long relaxation time [8]. Indeed, we did not always succeed in reaching equilibrium after only 10^4 MC steps; for the same

Table 1. Monte Carlo results for the fraction θ of sites occupied, the fluctuations in θ, the total adsorption Γ and the numbers m_1 and m_2 of particles per unit surface area in the first two layers. The estimated errors in $\Gamma\sigma^2$, $m_1\sigma^2$ and $m_2\sigma^2$ are respectively ± 0.08, ± 0.02 and ± 0.02.

$\exp(-\beta\varepsilon)$	θ	$(\langle\theta^2\rangle - \langle\theta\rangle^2)^{1/2}$	$\Gamma\sigma^2$	$m_1\sigma^2$	$m_2\sigma^2$
1	0.001	—	0.36	0.81	0.8
0.08	0.015 ± 0.002	0.0009	0.35	0.81	0.8
0.07	0.022 ± 0.004	0.013	0.35	0.81	0.81
0.06	0.027 ± 0.004	0.015	0.35	0.82	0.81
0.05	0.66 ± 0.01	0.055	0.54	1.02	0.79
0.03	0.79 ± 0.01	0.026	0.56	1.04	0.83
0.02	0.86 ± 0.01	0.020	0.55	1.047	0.83
0.01	0.93 ± 0.01	0.015	0.56	1.047	0.82
0	1	0	0.58	1.047	0.83

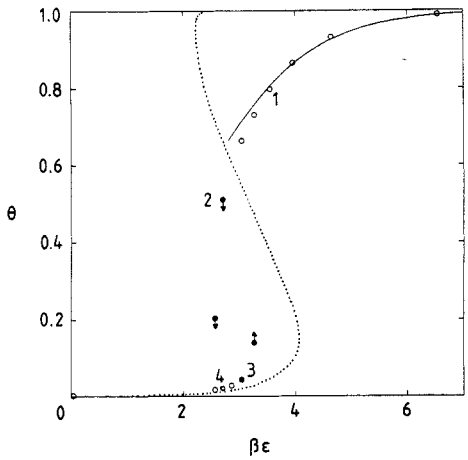

Figure 3. The fraction of sites occupied as a function of the site potential: ○ MC results for equilibrium states; ● MC points which are metastable (the arrow indicates the tendency of evolution; ····, Bragg–Williams approximation (18) with NN restriction; ———, Langmuir isotherm (20).

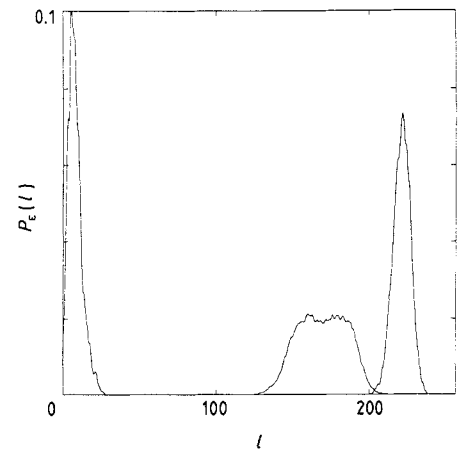

Figure 4. The MC probability $P_\varepsilon(l)$ of finding l sites occupied. From left to right, $\exp(-\beta\varepsilon) = 0.06$, 0.05 and 0.02.

value of ε, we found that the two series of configurations S_1 and S_2 gave different results for θ in a significant domain of $\beta\varepsilon$. In this region, we thus performed much longer runs (about 5×10^4 moves per particle) in order to eliminate the metastable states. To save computation time we occasionally stopped the calculation when a clear tendency towards an equilibrium state appeared. For $\beta\varepsilon = 3$, we found that the series S_1 remained locked at a low value of θ—which we believe to be metastable since the values for the two planes were not equal—while S_2 reached its equilibrium value in the dense phase. All the resulting points are indicated in figure 3.

The fluctuations in θ given in table 1 present a maximum at the transition, as expected. Accordingly, the probability distributions $P_\varepsilon(1)$ shown in figure 4 lose their nearly Gaussian shape near the transition and become flat and broader; in general this is the prelude to the appearance of two maxima. However, we never observed definite proof of the existence of a first-order transition in a simulation: the oscillation of metastable states between the two thermodynamical branches.

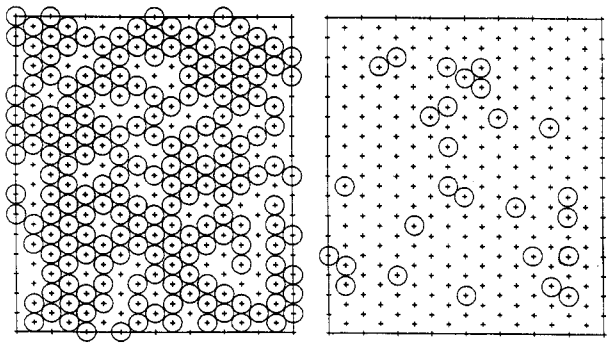

Figure 5. Snapshots of particle configurations: ((*a*) adsorbed atoms; (*b*) off-site atoms) in the region 0–0.1σ from the wall (point 1 in figure 3): ×, centres of the sites.

We note in table 1 that the variation in Γ at the transition is primarily due to the variation in the number of particles in the first layer, since m_2 remains almost constant in the full range of variation in $\beta\varepsilon$. Moreover, although θ changes significantly with $\beta\varepsilon$ in *each* phase, Γ and m_1 remain constant. A possible interpretation of these data and of the mechanism of the transition can be offered as follows.

Let us first consider the evolution along the upper branch. When $\varepsilon = \infty$, all the particles in the first layer are confined by the external field of the sites; the value $m_1 = 1.047\sigma^{-2}$ corresponds precisely to the completely filled lattice $(2/\sqrt{3}d^{-2})$. As ε is reduced, particles may leave their sites and θ decreases but, because of a second layer which is well localised at $z = \sigma$ (figure 2), they cannot move away from the wall and the first layer remains complete. This picture is confirmed by the 'snapshots' shown in figure 5 which represent the instantaneous configurations of the particles having their centres in the range $0 < z < 0.1\sigma$; we clearly see that most off-site particles stay very close to the sites and are likely to make only oscillatory moves around them. Another confirmation is given by the radial in-plane distribution function shown in figure 6; we observe that $g_r(R)$ takes significant values only near $R = R_{\alpha\beta}$, the site–site distances.

At the transition, the first and second layers are not so well defined, as seen in figure 2, and vertical displacements become possible for the adatoms. Therefore, when a particle moves away from the wall, the hole created in the first layer is no longer filled by particles of the second layer. This hole allows nearby adatoms to make larger lateral displacements and to leave their sites. These 'defects' increase their size and ultimately destroy the localised phase. The snapshots in figure 7 which correspond to a non-equilibrated configuration show how this 'melting' of the localised phase occurs.

The mechanism of the transition from the mobile phase may be best understood by examining the site–site pair distribution function represented in figure 8. We see that the shape of $g_{ss}(R_{\alpha\beta})$ changes dramatically as $\beta\varepsilon$ increases; the familiar oscillatory behaviour which corresponds to the structure of the initial fluid at $\varepsilon = 0$ is replaced by a monotonic curve which does not seem to go to 1—at least in the limited range of distances which can be investigated in our simulation box. Actually, it is the whole scale of the site–site distribution function which has changed. We may attribute this behaviour to the formation of 'clusters' on the

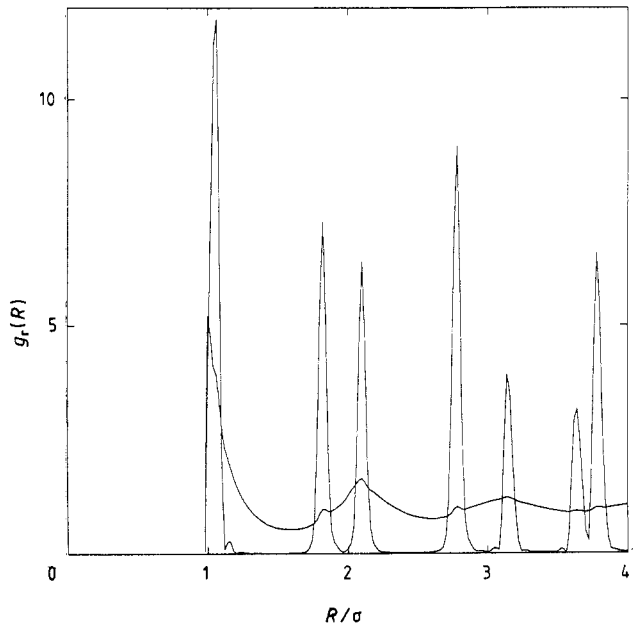

Figure 6. MC in-plane radial pair distribution function $g_r(R)$. The upper curve is for $\exp(-\beta\varepsilon) = 0.05$ and the lower curve for $\exp(-\beta\varepsilon) = 0.07$.

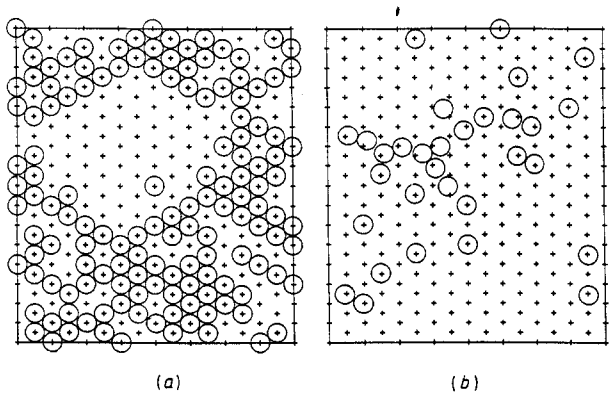

Figure 7. Same as figure 5 for point 2 in figure 3.

lattice like that displayed in figure 9. Of course, we see also in the same snapshot that most particles in the layer are off site, so that the corresponding radial distribution function (figure 6) has almost the usual aspect. This tendency of the adatoms to clustering was also observed in the preceding simulation [2] and it seems to justify the introduction of an effective attractive potential in the 2D lattice gas.

4. Discussion and conclusion

The 2D effective theory has predicted successfully the existence of a first-order phase transition in the adsorbed layer. Can it give us more information?

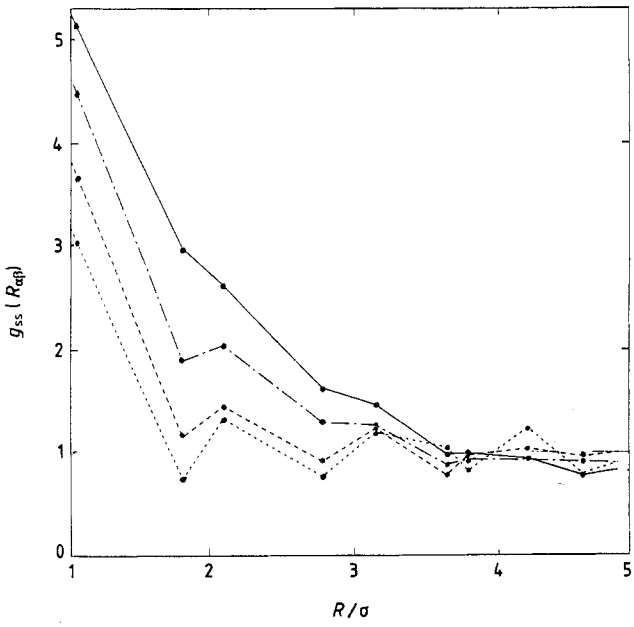

Figure 8. MC site–site pair distribution function $g_{ss}(R_{\alpha\beta})$. From bottom to top, $\exp(-\beta\varepsilon) = 1, 0.08, 0.06$ and 0.05 (metastable point 3 in figure 3). The lines are only a guide for the eye.

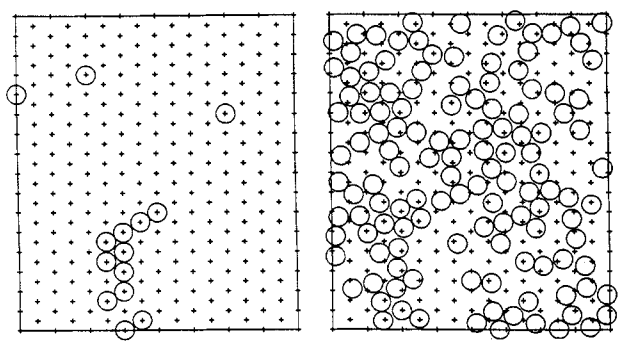

Figure 9. Same as figure 5 for point 4 in figure 3.

As seen in figure 3, the approximate Bragg–Williams isotherm (18), with the summation restricted to NN sites, is able to describe correctly the first points of the lower branch. More remarkably, it predicts also that the transition should occur at $\beta\varepsilon = 3.08$, which is in very good agreement with the MC result. However, this success should be viewed with some caution. In the first place we see in figure 10 that for $\eta_b = 0.46$ the effective pair potential $w_0^{av}(R)$ has a range of several molecular diameters so that the summation in (18) should not be restricted to NN sites; the consequence is a reduction in the amplitude of the overall effective potential which goes from $-1.3kT$ to $-1.1kT$. This would displace the transition towards $\beta\varepsilon = 3.6$. Secondly, and more important, the quite asymmetrical compositions of the coexistence phases at the transition (figure 3) invalidates the introduction of an effective *pairwise* potential amongst the lattice gas particles; in such a case the 2D isotherm θ_{2D} as a function of μ_{2D} should be symmetrical

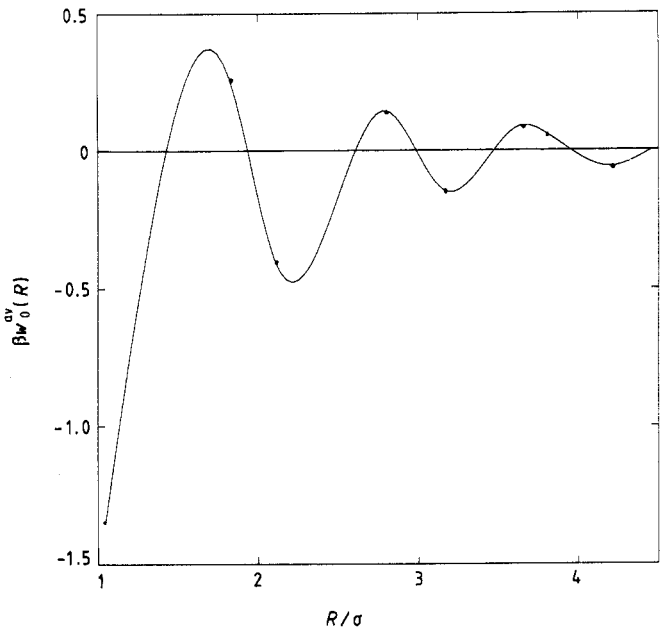

Figure 10. The effective potential $w_0^{av}(R)$. The points correspond to the site–site distances $R_{\alpha\beta}$.

about the mean value $\theta_{2D} = 0.5$. Even if we take into account the relation between θ and θ_{2D} (equation (9)) we cannot explain the behaviour displayed in figure 3 (incidentally, we see also in this figure that, because of (9), (18) does not warrant that θ remains smaller than 1). Such a failure may be the signature that three-body and higher-order interactions, neglected in the superposition approximation (10), play a significant role in the dense phase. This is not unexpected since the Kirkwood approximation for triplet correlations is known to break down at large densities ($\eta_b \geqslant 0.4$) in the bulk fluid [9]. This influence of n-body effects is also confirmed by inspection of the site–site pair distribution function $g_{ss}(R_{\alpha\beta})$ in the localised phase (as noted before, in the effective 2D theory this function can be identified with the pair distribution function of the lattice gas). We find that g_{ss} stays very close to 1 all along the upper branch; for instance $g_{ss}(d) = 1.01$ for $\theta = 0.86$ and $g_{ss}(d) = 1.04$ for $\theta = 0.66$. Therefore in this region the 2D fluid behaves as a free lattice gas and it appears that the n-body potentials $w_0^{(n)}(\boldsymbol{R}^n)$ in the original HW–HS interface have completely balanced the effect of the attractive two-body interaction. This overestimation of the effective potential for high coverage was already noticed in [3].

If there is no net interaction amongst the adatoms in the high coverage region, the upper branch of the isotherm should be well represented by the Langmuir equation (remember that $\theta \simeq \theta_{2D}$ for large $\beta\varepsilon$)

$$\theta/(1-\theta) = K\exp(\beta\varepsilon) \tag{20}$$

where K is some unknown parameter. Indeed, as seen in figure 3, we found that the choice $K = 0.12$ provides a good fit of the MC data. We have not been able to explain this precise value of K.

In conclusion, we have shown that the structure of an adsorbed layer at a liquid–solid interface is strongly influenced by the presence of the bulk liquid. Correlations in

the dense fluid may induce a cooperative behaviour in the layer even if the direct interactions between adatoms are only repulsive. This is in contrast with the case of adsorbed gas monolayers where the 3D nature of the interface does not play a major role in the properties of the adsorbed phase [10]. We have tried to incorporate this feature in an effective 2D theory, which has been only partially successful because of our limited knowledge of the correlation functions in the inhomogeneous hard-sphere fluid.

Acknowledgments

This work was supported in part by the Groupement de Recherche CNRS-ARTEP (wettability) and the Fond de Soutien des Hydrocarbures. Computer time on the VP200 at CIRCE was allocated by the Chemistry Department of CNRS. We are especially grateful to D Levesque (LPTHE, Orsay) for his great help in the numerical simulation.

References

[1] Badiali J P, Blum L and Rosinberg M L 1986 *Chem. Phys. Lett.* **129** 149
[2] Caillol J M, Levesque D and Weis J J 1987 *J. Chem. Phys.* **87** 6150
[3] Kierlik E and Rosinberg M L 1989 *Mol. Phys.* **68** 867
[4] Huckaby D A and Blum L 1990 *J. Chem. Phys.* at press
[5] Syozi I 1972 *Phase Transitions and Critical Phenomena* vol 1, ed C Domb and M S Green (New York: Academic) pp 269–329 and references therein
[6] Henderson D and Plischke M 1988 *J. Chem. Phys.* **92** 7177
[7] Verlet L and Weis J J 1972 *Phys. Rev.* A **5** 939
[8] Binder K 1987 *Rep. Prog. Phys.* **50** 783
[9] Parinello M and Giaquinta P V 1981 *J. Chem. Phys.* **74** 1990
[10] Nicholson D and Parsonage N G 1982 *Computer Simulation and the Statistical Mechanics of Adsorption* (London: Academic)